# Floquet Second-Order Topological Insulators from Nonsymmorphic Space-Time Symmetries

Yang Peng[1,2,*] and Gil Refael[1]

[1]*Institute of Quantum Information and Matter and Department of Physics, California Institute of Technology, Pasadena, California 91125, USA*

[2]*Walter Burke Institute for Theoretical Physics, California Institute of Technology, Pasadena, California 91125, USA*

We propose a systematic way of constructing Floquet second-order topological insulators (SOTIs) based on time-glide symmetry, a nonsymmorphic space-time symmetry that is unique in Floquet systems. In particular, we are able to show that the static enlarged Hamiltonian in the frequency domain acquires reflection symmetry, which is inherited from the time-glide symmetry of the original system. As a consequence, one can construct a variety of time-glide symmetric Floquet SOTIs using the knowledge of static SOTIs. Moreover, the time-glide symmetry only needs to be implemented approximately in practice, enhancing the prospects of experimental realizations. We consider two examples, a 2D system in class AIII and a 3D system in class A, to illustrate our ideas, and then present a general recipe for constructing Floquet SOTIs in all symmetry classes.

*Introduction.*—Symmetry and topology are both at the crux of topological phases. Nonspatial symmetries, i.e., time-reversal (TR), particle-hole, and chiral symmetries, allow a classification of topological insulators and superconductors into one of the ten Altland-Zirnbauer (AZ) symmetry classes [1–5]. When additional spatial symmetries are considered, the classification can be enriched, giving rise to weak topological insulators (TIs) [6] protected by lattice translational symmetry, as well as the topological crystalline insulators [6,7], protected by crystalline symmetries.

Recently, the idea of utilizing crystalline symmetries was used to construct and understand a new family of TIs: the higher-order TIs [8–14]. An $n$th-order TI in $d$ dimensions will have topologically protected gapless modes that live in the $(d - n)$-dimensional boundaries, but all $(d - n')$ boundaries with $n' > n$ are gapped. Thus, the conventional TIs are first-order TIs according to this definition, while the second-order TIs (SOTIs) in two and three dimensions will host protected zero energy corner modes and gapless hinge modes, respectively.

On the other hand, topological phases also exist under nonequilibrium conditions and can be realized by time-periodic driving, known as Floquet engineering. For instance, a Floquet TI with chiral edge modes can be brought from a static band insulator by applying a periodic drive, such as a circularly polarized radiation or an alternating Zeeman field [15–19]. Thus, it is natural to ask, how can higher-order TIs be generated with Floquet engineering? Recently, specific examples of such systems were introduced in Refs. [20–22].

In this work, we provide a general recipe of constructing Floquet second-order TIs in all symmetry classes, by making use of the dynamical nature and the time dimension in a Floquet system. In particular, we construct Floquet SOTIs from an approximate time-glide symmetry [23], a specific nonsymmorphic space-time crystalline symmetry [24], which is unique in a time-periodic system and has no static analog.

The basic principle behind our construction is as follows. The $(d - 1)$-dimensional boundaries in the Floquet SOTIs are essentially stand-alone $(d - 1)$ Floquet insulators from a topological perspective, similar to their static cousin [10]. Hence, topologically protected corner $(d = 2)$ or hinge $(d = 3)$ modes naturally become domain-wall excitations at the intersection of two gapped boundaries, if these fall into different topological phases. The approximate space-time symmetry then crucially protects such domain walls.

The use of space-time symmetries in Floquet engineering of SOTIs may offer certain advantages over other recipes of creating SOTIs based only on spatial point group symmetries. Using external time-dependent fields may remove stringent requirements on material structure, and introduce more controllability. To wit, space-time symmetries can be induced externally, by applying alternating fields which change directions every half a period. Moreover, these space-time symmetries need only be approximately implemented, further enhancing prospects for experimental realizations.

*Floquet second-order topological insulators with time-glide symmetry.*—The corner and edge modes in a Floquet SOTI actually follow the classification of one- and two-dimensional Floquet topological insulators; see Refs. [25,26], for example. Thus, we only have Floquet SOTIs in certain AZ symmetry classes, as shown in Table I, where we have listed

the topological invariants for each quasienergy gap. Note that these invariants in $d$ dimensions are exactly the same as the ones in a Floquet topological insulator in $d - 1$ dimensions. We will show in the following that it is possible to construct Floquet SOTI systematically in all five nontrivial AZ classes, based on a single time-glide symmetry $\mathcal{M}$, which ensures the presence of topologically protected corner or edge states.

The time-glide symmetry is a nonsymmorphic space-time symmetry, which is composed of a spatial reflection and a half-period time translation [23,24]. Without loss of generality, let us focus on the situation where the reflection plane within the time glide is perpendicular to $x$. When the symmetry acts on the Bloch Hamiltonian $H(k_x, \mathbf{k}_\parallel, t)$, where $k_\parallel$ denotes the rest Bloch momenta parallel to the reflection plane, we have

$$\mathcal{M}H(k_x, \mathbf{k}_\parallel, t)\mathcal{M} = H(-k_x, \mathbf{k}_\parallel, t + T/2), \qquad (1)$$

where $\mathcal{M}$ is the operator implementing the time-glide symmetry, which is both unitary and Hermitian.

A complete classification of time-glide symmetric Floquet topological insulators and superconductors in all AZ classes has been worked out in Ref. [23]. It was shown that when the edge is mapped onto itself by the reflection part of the time-glide operation, it can host protected anomalous Floquet gapless modes [27,28], even though the classification of the Floquet system without the time-glide symmetry is trivial. The existence of these anomalous Floquet modes is distinct from the modes protected by the spatial reflection symmetry in topological crystalline insulators, and is purely due to the space-time dynamical symmetry which has no static counterpart.

By deploying the dynamical time-glide symmetry, we can construct intrinsically nonequilibrium Floquet SOTIs with anomalous corner or hinge modes. Our recipe follows three rules, similar to the ones for constructing static SOTIs [10]. First, we require that one or more pairs of system boundaries are mapped onto each other by the reflection part of the time-glide operation. Second, the topological classification will be trivial when the time-glide symmetry is broken. Third, the classification of the corresponding AZ class in $(d - 1)$ dimensions must be nontrivial. This guarantees that the time-glide-symmetry-breaking mass, which gaps the glide-protected boundaries, is unique.

In Table I, we list all the Floquet SOTIs that can be constructed according to the above recipe. In the rest of the Letter, we will construct examples of Floquet SOTIs hosting anomalous Floquet corner or hinge modes, namely the modes with quasienergies inside the bulk gap at the Floquet zone boundaries.

Our construction of Floquet SOTIs uses the frequency-domain formulation of the Floquet problem [27]. In this formulation, the quasienergies $\{\epsilon_j\}$ result from diagonalizing the enlarged Hamiltonian $\mathcal{H}(\mathbf{k})$, whose matrix blocks are given by $H(\mathbf{k}, t)$ as $\mathcal{H}_{mm'}(\mathbf{k}) = m\omega\delta_{mm'}\mathbb{I} + H_{m'-m}(\mathbf{k})$,

TABLE I. The AZ symmetry classes are defined by the presence ($\pm 1$) or absence (0) of time-reversal $\mathcal{T}$, particle-hole $\mathcal{C}$, and chiral symmetry $\mathcal{S}$. The values $\pm 1$ correspond to $\mathcal{T}^2$, $\mathcal{C}^2$, or $\mathcal{S}^2$. The topological invariants at a particular quasienergy gap for the two-dimensional and three-dimensional Floquet SOTIs, which can be constructed from time-glide symmetric Floquet topological phases, are listed in last four columns, as well as the time-glide symmetry $\mathcal{M}$. The symbols $\mathcal{M}_{\eta_S}$, $\mathcal{M}_{\eta_T}$, $\mathcal{M}_{\eta_C}$, and $\mathcal{M}_{\eta_T\eta_C}$ refer to a time-glide operator that squares to one and commutes ($\eta = +$) or anticommutes ($\eta = -$) with $\mathcal{S}$, $\mathcal{T}$, and $\mathcal{C}$; i.e., $\mathcal{M}\mathcal{S} = \eta_S\mathcal{S}\mathcal{M}$, $\mathcal{M}\mathcal{T} = \eta_T\mathcal{T}\mathcal{M}$, and $\mathcal{M}\mathcal{C} = \eta_C\mathcal{C}\mathcal{M}$.

| Class | $\mathcal{T}$ | $\mathcal{C}$ | $\mathcal{S}$ | $d = 2$ | | $d = 3$ | |
|-------|------|------|------|---------|---|---------|---|
| A | 0 | 0 | 0 | $\cdots$ | 0 | $\mathcal{M}$ | $\mathbb{Z}$ |
| AIII | 0 | 0 | 1 | $\mathcal{M}_-$ | $\mathbb{Z}$ | $\cdots$ | 0 |
| AI | 1 | 0 | 0 | $\cdots$ | 0 | $\cdots$ | 0 |
| BDI | 1 | 1 | 1 | $\mathcal{M}_{+-}$ | $\mathbb{Z}$ | $\cdots$ | 0 |
| D | 0 | 1 | 0 | $\mathcal{M}_-$ | $\mathbb{Z}_2$ | $\mathcal{M}_-$ | $\mathbb{Z}$ |
| DIII | $-1$ | 1 | 1 | $\mathcal{M}_{+-}, \mathcal{M}_{-+}, \mathcal{M}_{--}$ | $\mathbb{Z}_2$ | $\mathcal{M}_{+-}, \mathcal{M}_{--}$ | $\mathbb{Z}_2$ |
| AII | $-1$ | 0 | 0 | $\cdots$ | 0 | $\mathcal{M}_+, \mathcal{M}_-$ | $\mathbb{Z}_2$ |
| CII | $-1$ | $-1$ | 1 | $\mathcal{M}_{+-}, \mathcal{M}_{-+}$ | $2\mathbb{Z}$ | $\cdots$ | 0 |
| C | 0 | $-1$ | 0 | $\cdots$ | 0 | $\mathcal{M}_-, \mathcal{M}_+$ | $2\mathbb{Z}$ |
| CI | 1 | $-1$ | 1 | $\cdots$ | 0 | $\cdots$ | 0 |

with $H_n(\mathbf{k}) = (1/T) \int_0^T dt H(\mathbf{k}, t)e^{-in\omega t}$. Here $\mathbb{I}$ is the identity matrix of the same dimension as $H(\mathbf{k})$, and $m, m', n \in \mathbb{Z}$. Moreover, quasienergies $\epsilon_j$ and $\epsilon_j + m\omega$ describe the same physical state, and only quasienergies within a single interval of $\omega$, e.g., the "first Floquet zone" with $-\omega/2 < \epsilon_j < \omega/2$, are unique.

To obtain a low-energy effective theory of the anomalous Floquet SOTIs, we should focus on gapless edge modes near $\epsilon = \omega/2$ (modulo $\omega$), similar to the static case where one assumes a Dirac-like low-energy theory. These states would always be a result of the time-dependent drive. For that, we focus on a $2 \times 2$ block of $\mathcal{H}$ containing the two Floquet zones shifted by $(2n + 1)\omega$, with some $n \in \mathbb{Z}$; namely,

$$\mathcal{H}_{\text{eff}} = \begin{pmatrix} H_0 + (n + \frac{1}{2})\omega & H_{2n+1} \\ H_{2n+1}^\dagger & H_0 - (n + \frac{1}{2})\omega \end{pmatrix} + \frac{\omega}{2}\rho_0, \quad (2)$$

with $\rho_0$ the identity in the two Floquet zone basis. This describes the situation where the bottom band of $H_0 + (n + 1)\omega$ crosses the top band of $H_0 - n\omega$, and $H_{2n+1}$ opens a bulk gap at the crossing. The last term in Eq. (2) shifts the energy origin of the problem by $\omega/2$. What remains of $\mathcal{H}_{\text{eff}}(\mathbf{k})$ is a reflection-symmetric system, with the effective reflection symmetry operator $\mathcal{R}_{\text{eff}} = \rho_z \otimes \mathcal{M}$, where $\rho_{x,y,z}$ are the Pauli matrices in the space of the two Floquet zones. Hence, we have mapped a Floquet system with a time-glide symmetry to a static system with a reflection symmetry within the effective description of the anomalous Floquet edge modes.

Based on the Hamiltonian Eq. (2), we construct lattice models for harmonically driven SOTIs of the form

$$H(\mathbf{k}, t) = H_0(\mathbf{k}) + H_1(\mathbf{k})e^{i\omega t} + H_1^{\dagger}(\mathbf{k})e^{-i\omega t}, \quad (3)$$

which couples the upper bands of $H_0 + \omega$ to the lower bands of $H_0$, corresponding to the $n = 0$ case of $\mathcal{H}_{\text{eff}}$ of Eq. (2). $H_{0,1}(\mathbf{k})$ respect the time-glide symmetry, as well as the nonspatial class-appropriate AZ symmetries.

Before we proceed, it is important to note that terms that gap the anomalous Floquet gapless modes when time-glide symmetry is broken are odd under the time-glide operation (crucially, such terms arise when edges are not locally symmetric under the mirror element of the glide). Hence, the masses in the quasienergy spectra of the two $(d-1)$ boundaries, which are connected via the time-glide operation, will generically give rise to $(d-2)$ boundary modes. One can, therefore, break the time-glide symmetry and still have protected $(d-2)$ boundary modes as long as the gaps of the bulk and the $(d-1)$ boundaries do not close. Hence, the time-glide symmetry need only be implemented approximately, which greatly enhances the prospects of an experimental realization.

*Two-dimensional Floquet SOTI in class AIII.*—For a Floquet system in class AIII in 2D with a time-periodic Bloch Hamiltonian $H(k_x, k_y, t) = H(k_x, k_y, t + T)$ of period $T$, chiral and time-glide symmetry operators $\mathcal{S}$ and $\mathcal{M}$ obey $\mathcal{S}H(k_x, k_y, t) = -H(k_x, k_y, -t)\mathcal{S}$ and $\mathcal{M}H(k_x, k_y, t) = H(-k_x, k_y, t + T/2)\mathcal{M}$. Without the time-glide symmetry, 2D Floquet insulators are trivial. When, however, the time-glide symmetry anticommutes with $\mathcal{S}$, such systems support a $\mathbb{Z}$ classification.

The effective Hamiltonian defined in Eq. (2) describes a reflection-symmetric system in class AIII, with an effective chiral symmetry $\mathcal{S}_{\text{eff}} = \rho_x \otimes \mathcal{S}$. When $\{\mathcal{M}, \mathcal{S}\} = 0$, we have $[\mathcal{S}_{\text{eff}}, \mathcal{R}_{\text{eff}}] = 0$, which leads to a $\mathbb{Z}$ topological classification and can give rise to helical edge modes [29,30] at the reflection-symmetric edge.

Indeed, the anomalous edge state perpendicular to the time-glide plane can be characterized by an edge Hamiltonian $H_{\text{edge}}(k_x) = \omega/2 + k_x\Gamma_x$, where the edge-mode velocity was rescaled to 1, and $\Gamma_x$ describes a number of helical modes, and satisfies $\Gamma_x^2 = 1$. Because of the presence of $\mathcal{S}_{\text{eff}}$ and $\mathcal{R}_{\text{eff}}$, we have $[\Gamma_x, \mathcal{S}_{\text{eff}}\mathcal{R}_{\text{eff}}] = 0$. Hence, $\Gamma_x$ and $\mathcal{S}_{\text{eff}}\mathcal{R}_{\text{eff}}$ can be simultaneously diagonalized. Suppose we can add a mass term $\Gamma_m$ that respects both the effective chiral and reflection symmetries. Then we have $\{\Gamma_m, \mathcal{S}_{\text{eff}}\mathcal{R}_{\text{eff}}\} = 0$, indicating that $\Gamma_m$ can only gap out helical modes with opposite eigenvalues of $\mathcal{S}_{\text{eff}}\mathcal{R}_{\text{eff}}$. Thus, the $\mathbb{Z}$ topological index actually counts the difference between the number of helical edge states with positive and negative eigenvalue of $\mathcal{S}_{\text{eff}}\mathcal{R}_{\text{eff}}$.

Let us consider, for instance, the helical states with $\mathcal{S}_{\text{eff}}\mathcal{R}_{\text{eff}} = 1$. The reflection operation here is effectively the same as the chiral symmetry operation; namely,
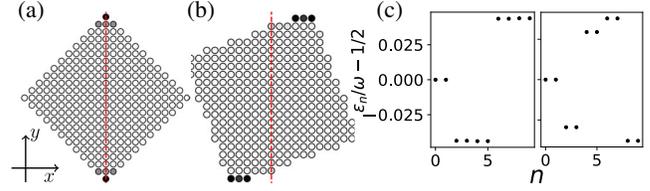


FIG. 1. (a),(b) Support of the anomalous Floquet corner modes (darker for a larger magnitude) at quasienergy $\omega/2$ obtained from exact diagonalization of the enlarged Hamiltonian $\mathcal{H}$ (truncated up to $H_0 \pm 2\omega$) for the two-dimensional class AIII system with time-glide symmetry defined in Eq. (3), with $\omega = 6$, $m = 4$, $b = 0.4$, $b' = 0.8$ (reflection-symmetry-breaking term). The red dashed line indicates the time-glide plane. (c) The ten eigenvalues closest to $\omega/2$ for the two systems are shown.

$\mathcal{R}_{\text{eff}} = \mathcal{S}_{\text{eff}}$. If we further consider a spatial configuration with an edge that breaks the effective reflection symmetry, a mass $\Gamma_m$ that preserves the chiral symmetry, with $\{\Gamma_m, \mathcal{R}_{\text{eff}}\} = 0$ and $\{\Gamma_m, \Gamma_x\} = 0$, can be added to the edge Hamiltonian. In particular, those edges which are connected via the reflection operation will have opposite mass. Since class AIII in one dimension has a $\mathbb{Z}$ topological invariant, the mass is unique. Thus, the intersection of two reflection-related edges corresponds to a domain wall for the edge theory, which harbors an anomalous Floquet localized state at $\omega/2$.

A lattice model that realizes such a Floquet SOTI follows the form of Eq. (3), with $H_0(\mathbf{k}) = (m - \cos k_x - \cos k_y)\tau_z + b\sigma_z$, and $H_1(\mathbf{k}) = (\sin k_y \sigma_y - i \sin k_x)\tau_-$. Here $\sigma_{x,y,z}$ and $\tau_{x,y,z}$ are the two sets of Pauli matrices for this four-band model, and $\tau_{\pm} = (\tau_x \pm i\tau_y)/2$. The chiral and time-glide symmetries are realized by $\mathcal{S} = \tau_x\sigma_x$, $\mathcal{M} = \sigma_z$.

The corresponding effective Hamiltonian $\mathcal{H}_{\text{eff}}$ of Eq. (2) with $n = 0$ is actually block diagonalized into two blocks with $\rho_z\tau_z = \pm 1$. The block with $\rho_z\tau_z = 1$ is actually a trivial band insulator, whereas the one with $\rho_z\tau_z = -1$ describes a reflection symmetry topological insulator with helical modes on the edge parallel to $x$ around momentum $k_x = 0$ for $(m - \omega/2) \in (0, 2)$, and around momentum $k_x = \pi$ for $(m - \omega/2) \in (-2, 0)$, where $b$ is numerically small. In these parameter regimes, if we cut the system such that the two edges are mapped into each other via the reflection with respect to the time-glide plane, we expect to find corner modes at their intersections. Note that this model also has a reflection symmetry implemented by $\tau_z\sigma_z$. One can actually introduce an additional term $b'\tau_y$ that breaks this reflection symmetry without affecting the corner modes, as shown in the numerics.

Figure 1(a) depicts these states, alongside the quasienergies close to $\omega/2$ in Fig. 1(c). Even boundaries that completely break time-glide symmetry, as in Fig. 1(b), still give rise to localized corner modes, which are still pinned to $\omega/2$ and separated by a smaller gap from the states at other quasienergies; see Fig. 1(c). Thus, the presence of anomalous corner modes does not rely on the time-glide symmetry.

It is worth mentioning that a time-glide symmetric Floquet SOTI can also be constructed using a two-step drive, which may be easier to implement experimentally. For example, let us consider a system driven by two static Hamiltonians $H_\pm$ in each half period, defined as

$$H_\pm = \cos k_x \tau_x + \sin k_x \tau_y + J(\cos k_y \sigma_x \pm \sin k_y \tau_y \sigma_y), \quad (4)$$

where the chiral and the time-glide (with reflection of the $x$ direction) symmetries are realized by $\mathcal{S} = \tau_z \sigma_z$ and $\mathcal{M} = \tau_x$. It was shown in Ref. [23] that this system can also host anomalous Floquet helical edge modes protected by the time-glide symmetry. If the system contains a pair of edges which are approximately reflected onto each other by the time-glide symmetry, as in Figs. 1(a) and 1(b), anomalous Floquet corner modes appear at the intersections (see Supplemental Material [31]).

*Three-dimensional Floquet SOTI in class A.*—Without time-glide symmetry, 3D Floquet systems in class A are topologically trivial. Imposing a time-glide symmetry (realized by $\mathcal{M}$) gives rise to anomalous Floquet surface modes. Consider the effective Hamiltonian $\mathcal{H}_{\mathrm{eff}}$ given in Eq. (2). Then $\mathcal{H}_{\mathrm{eff}}$ describes a class A system with an additional reflection symmetry $\mathcal{R}_{\mathrm{eff}}$, which allows for a $\mathbb{Z}$ mirror Chern number enumerating gapless surface states at reflection-symmetric surfaces [29,30].

The surface Hamiltonian describing the gapless modes on the plane normal to the $z$ direction can be written as $H_{\mathrm{surface}} = \omega/2 + k_x \Gamma_x + k_y \mathcal{R}_{\mathrm{eff}}$, with $\{\Gamma_x, \mathcal{R}_{\mathrm{eff}}\} = 0$. A reflection-symmetry-breaking mass $\Gamma_m$, with $\{\Gamma_m, \mathcal{R}_{\mathrm{eff}}\} = 0$ and $\{\Gamma_m, \Gamma_x\} = 0$, will gap the surface. This mass is unique as class A in 2D has a nontrivial topological classification.

A 3D model also arises here by embedding a static ($x$ direction) reflection-symmetric system into $\mathcal{H}_{\mathrm{eff}}$. Using the form in Eq. (3), with $H_0(\mathbf{k}) = (m - \sum_{j=x,y,z} \cos k_j)\tau_z + b\sigma_x$ and $H_1(\mathbf{k}) = \sum_{j=x,y,z} \sin k_j \sigma_j \tau_-$, yields a 3D Floquet SOTI, with time-glide symmetry $\mathcal{M} = \sigma_x$.

When $(m - \omega/2) \in (1, 3)$, and $b$ numerically small, the $\rho_z \tau_z = -1$ block of $\mathcal{H}_{\mathrm{eff}}$ [of the form of Eq. (2)] is a 3D reflection-symmetric topological crystalline insulator in class A, with a gapless surface mode on the boundary normal to $x$. When we have two surfaces related by the reflection symmetry, a localized hinge mode appears at the intersection of the two surfaces. This corresponds to the anomalous Floquet modes of the full harmonically driven system. Similar to the class AIII case, this model also has a reflection symmetry implemented by $\tau_z \sigma_x$. One can get rid of this symmetry by invoking $b_1 \tau_x$, $b_2 \tau_y$, etc., without affecting the hinge modes.

Figure 2(a) presents a computation of the quasienergies of the Floquet hinge mode as a function of momentum $k_z$, with periodic boundary conditions assumed along the $z$ direction. In Fig. 2(b), the support of the hinge mode at $k_z = 0$ was shown. When we consider a finite cube, where
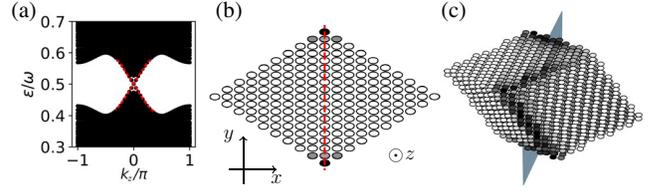


FIG. 2. (a) Bulk (black) and hinge (red) Floquet band structure near $\omega/2$ obtained from exact diagonalization of the enlarged Hamiltonian $\mathcal{H}$ (truncated up to $H_0 \pm 2\omega$) at each momentum along $z$ (periodic boundary condition), for the three-dimensional harmonically driven Floquet system in class A, with time-glide symmetry. The parameters are $\omega = 10$, $m = 7$, $b = 0.4$. (b) Support of the anomalous Floquet hinge modes at $k_z = 0$ at quasienergy $\omega/2$. (c) Support of the hinge modes with open boundary conditions along all directions. Here all surfaces break the reflection symmetry about the time-glide plane, which is shown in blue.

all surfaces generically break the reflection symmetry around the time-glide plane, as in Fig. 2(c), we see that the chiral Floquet hinge mode zigzags along certain hinges of the cube, as in the static 3D class A SOTI [10].

*Floquet SOTI in real symmetry classes.*—As we claimed above, the recipe of constructing Floquet SOTIs is completely general and can also be applied to real symmetry classes with time-reversal $\mathcal{T}$ and/or particle-hole (PH) $\mathcal{C}$ symmetries, which give rise to an effective TR $\mathcal{T}_{\mathrm{eff}} = \rho_0 \otimes \mathcal{T}$ or/and an effective PH $\mathcal{C}_{\mathrm{eff}} = \rho_x \otimes \mathcal{C}$ symmetry on the frequency-domain effective Hamiltonian $\mathcal{H}_{\mathrm{eff}}$ defined in Eq. (2).

For a system with time-glide symmetry $\mathcal{M}_{\eta_T, \eta_C}$, where $\eta_T, \eta_C$ characterizes the commutation relation between time glide, and the TR and PH, if they exist, namely, $\mathcal{MT} = \eta_T \mathcal{TM}$, $\mathcal{MC} = \eta_C \mathcal{CM}$. This determines the commutation relations between the effective reflection $\mathcal{R}_{\mathrm{eff}}^{\sigma_T, \sigma_C}$ and effective TR and PH, with $\sigma_T$ and $\sigma_C$ defined similarly as $\mathcal{R}_{\mathrm{eff}} \mathcal{T}_{\mathrm{eff}} = \sigma_T \mathcal{T}_{\mathrm{eff}} \mathcal{M}_{\mathrm{eff}}$, $\mathcal{M}_{\mathrm{eff}} \mathcal{C}_{\mathrm{eff}} = \sigma_C \mathcal{C}_{\mathrm{eff}} \mathcal{M}_{\mathrm{eff}}$. It is easy to show that $\sigma_T = \eta_T$ and $\sigma_C = -\eta_C$. In fact, Table I is the same as Table I in Ref. [10], if we replace $\mathcal{R}$ by $\mathcal{M}$ while taking into account the modification of commutation relations. Hence, a topological property of the quasienergy gap at the Floquet zone boundary in a time-glide symmetric Floquet system can be obtained from analyzing the corresponding reflection-symmetric static system in the same symmetry class, according to the mapping defined above.

To construct time-glide symmetric Floquet SOTIs using harmonic drives, let us start with a general $d$-dimensional static SOTI Hamiltonian of the form [32] $h(\mathbf{k}) = \sum_{j=0}^{d} d_j(\mathbf{k}) \Gamma_j + bB$, where $d_0(\mathbf{k}) = m + \sum_{j=1}^{d}(1 - \cos k_j)$, and for $j = 1, \ldots, d$, $d_j(\mathbf{k}) = \sin k_j$. Here the matrices $\Gamma_0$ and $\Gamma_j$s are mutually anticommuting, and $B$ commutes with $\Gamma_{0,1}$ but anticommutes with the rest of the $\Gamma_j$'s, which ensures for small $b$ that this Hamiltonian describes a topological crystalline phase with reflection symmetry in the first coordinate. One can choose $\Gamma_0 = \tau_z$, and embed $h$

into the $\rho_z \tau_z = -1$ block of $\mathcal{H}_{\text{eff}}$, with $m \to m - \omega/2$. This will give rise to a harmonically driven Floquet SOTI of the form described in Eq. (3) in the same AZ class of $h(\mathbf{k})$.

*Conclusion.*—In this work, we extend the second-order topological phase to the Floquet scenario. Particularly, we show how to systematically construct Floquet SOTIs based on time-glide symmetry, which is a nonsymmorphic space-time symmetry unique to Floquet systems.

When a pair of boundaries in the system, which defy the mirror symmetry, are approximately related via the reflection about the time-glide plane, a Floquet corner or hinge mode can appear at the intersection. This can be understood in the frequency-domain formulation of the Floquet system, by focusing on the effective two-by-two block of the enlarged Hamiltonian. We showed that this effective Hamiltonian acquires a reflection symmetry inherited from the time-glide symmetry, besides the AZ symmetries.

Thus, the properties of the time-glide symmetric Floquet SOTI can be understood from our previous knowledge of the static reflection symmetry SOTI [10]. Furthermore, we are able to systematically construct explicit models of harmonically driven time-glide symmetric Floquet SOTI, from Hamiltonians of static SOTIs. In addition to two examples (2D class AIII and a 3D class A systems), we showed that our recipe yields Floquet SOTIs in other symmetry classes. Since the lattice vibrations naturally break the static reflection symmetry while preserving the time-glide symmetry, we can expect to create Floquet SOTIs by exciting a particular phonon mode [33,34]. On the other hand, the phonons can also used as a heat bath to prevent the system from heating [35,36].

For other nonsymmorphic space-time symmetries that may give rise to Floquet higher-order topological insulators, our frequency-domain analysis can be applied and the knowledge of static systems with other crystalline symmetries can be used similarly. We intend to pursue these directions in our future work.

[*]Corresponding author.
yangpeng@caltech.edu

[1] A. P. Schnyder, S. Ryu, A. Furusaki, and A. W. W. Ludwig, Phys. Rev. B **78**, 195125 (2008).
[2] A. Kitaev, AIP Conf. Proc. **1134**, 22 (2009).
[3] S. Ryu, A. P. Schnyder, A. Furusaki, and A. W. Ludwig, New J. Phys. **12**, 065010 (2010).
[4] J. C. Y. Teo and C. L. Kane, Phys. Rev. B **82**, 115120 (2010).
[5] C.-K. Chiu, J. C. Y. Teo, A. P. Schnyder, and S. Ryu, Rev. Mod. Phys. **88**, 035005 (2016).
[6] L. Fu, Phys. Rev. Lett. **106**, 106802 (2011).
[7] Y. Ando and L. Fu, Annu. Rev. Condens. Matter Phys. **6**, 361 (2015).
[8] W. A. Benalcazar, B. A. Bernevig, and T. L. Hughes, Phys. Rev. B **96**, 245115 (2017).
[9] Y. Peng, Y. Bao, and F. von Oppen, Phys. Rev. B **95**, 235143 (2017).
[10] J. Langbehn, Y. Peng, L. Trifunovic, F. von Oppen, and P. W. Brouwer, Phys. Rev. Lett. **119**, 246401 (2017).
[11] W. A. Benalcazar, B. A. Bernevig, and T. L. Hughes, Science **357**, 61 (2017).
[12] Z. Song, Z. Fang, and C. Fang, Phys. Rev. Lett. **119**, 246402 (2017).
[13] F. Schindler, A. M. Cook, M. G. Vergniory, Z. Wang, S. S. Parkin, B. A. Bernevig, and T. Neupert, Sci. Adv. **4**, eaat0346 (2018).
[14] F. Schindler, Z. Wang, M. G. Vergniory, A. M. Cook, A. Murani, S. Sengupta, A. Y. Kasumov, R. Deblock, S. Jeon, I. Drozdov *et al.*, Nat. Phys. **14**, 918 (2018).
[15] T. Oka and H. Aoki, Phys. Rev. B **79**, 081406(R) (2009).
[16] J.-i. Inoue and A. Tanaka, Phys. Rev. Lett. **105**, 017401 (2010).
[17] T. Kitagawa, T. Oka, A. Brataas, L. Fu, and E. Demler, Phys. Rev. B **84**, 235108 (2011).
[18] N. H. Lindner, G. Refael, and V. Galitski, Nat. Phys. **7**, 490 (2011).
[19] N. H. Lindner, D. L. Bergman, G. Refael, and V. Galitski, Phys. Rev. B **87**, 235131 (2013).
[20] B. Huang and W. V. Liu, arXiv:1811.00555.
[21] R. W. Bomantara, L. Zhou, J. Pan, and J. Gong, Phys. Rev. B **99**, 045441 (2019).
[22] M. Rodriguez-Vega, A. Kumar, and B. Seradjeh, arXiv:1811.04808.
[23] T. Morimoto, H. C. Po, and A. Vishwanath, Phys. Rev. B **95**, 195155 (2017).
[24] S. Xu and C. Wu, Phys. Rev. Lett. **120**, 096401 (2018).
[25] R. Roy and F. Harper, Phys. Rev. B **96**, 155118 (2017).
[26] S. Yao, Z. Yan, and Z. Wang, Phys. Rev. B **96**, 195303 (2017).
[27] M. S. Rudner, N. H. Lindner, E. Berg, and M. Levin, Phys. Rev. X **3**, 031005 (2013).
[28] F. Nathan and M. S. Rudner, New J. Phys. **17**, 125014 (2015).
[29] C.-K. Chiu, H. Yao, and S. Ryu, Phys. Rev. B **88**, 075142 (2013).
[30] K. Shiozaki and M. Sato, Phys. Rev. B **90**, 165114 (2014).
[31] See Supplemental Material at http://link.aps.org/supplemental/10.1103/PhysRevLett.123.016806 for more details. In this, we introduce a model for the Floquet SOTI in class AIII under a two-step drive. Additionally, we show how the does the time-glide symmetry appear as the reflection symmetry in the frequency-domain formulation of the Floquet problem.
[32] M. Geier, L. Trifunovic, M. Hoskam, and P. W. Brouwer, Phys. Rev. B **97**, 205135 (2018).

[33] T. F. Nova, A. Cartella, A. Cantaluppi, M. Först, D. Bossini, R. Mikhaylovskiy, A. Kimel, R. Merlin, and A. Cavalleri, Nat. Phys. **13**, 132 (2017).

[34] H. Hubener, U. De Giovannini, and A. Rubio, Nano Lett. **18**, 1535 (2018).

[35] K. I. Seetharam, C.-E. Bardyn, N. H. Lindner, M. S. Rudner, and G. Refael, Phys. Rev. X **5**, 041050 (2015).

[36] K. I. Seetharam, C.-E. Bardyn, N. H. Lindner, M. S. Rudner, and G. Refael, Phys. Rev. B **99**, 014307 (2019).